remote sensing

MDPI

Article

A Comprehensive Assessment of Climate Change and Anthropogenic Effects on Surface Water Resources in the Lake Urmia Basin, Iran

Mohammad Kazemi Garajeh [1,2], Rojin Akbari [3], Sepide Aghaei Chaleshtori [4], Mohammad Shenavaei Abbasi [5], Valerio Tramutoli [2,*], Samsung Lim [6] and Amin Sadeqi [7]

1 Department of Civil, Constructional and Environmental Engineering, Sapienza University of Rome, 00185 Rome, Italy; mohammad.kazemigarajeh@uniroma1.it
2 School of Engineering, Università degli Studi della Basilicata, Via Nazario Sauro 85, 85100 Potenza, Italy
3 Department of Natural Resources Engineering, Isfahan University of Technology, Isfahan 84156-83111, Iran; rojin.akbari@alumni.iut.ac.ir
4 Department of Irrigation, College of Agriculture, Isfahan University of Technology, Isfahan 84156-8311, Iran; s.aghaei@alumni.iut.ac.ir
5 Department of Engineering and Natural Sciences, Faculty of Materials Science and Environmental Engineering, Tampere University, 33014 Tampere, Finland; mohammad.shenavaeiabbasi@tuni.fi
6 School of Civil and Environmental Engineering, University of New South Wales, Sydney 2052, Australia; s.lim@unsw.edu.au
7 Department of Geography and Geology, University of Turku, 20014 Turku, Finland; amin.sadeqi@utu.fi
* Correspondence: valerio.tramutoli@unibas.it

Abstract: In recent decades, the depletion of surface water resources within the Lake Urmia Basin (LUB), Iran, has emerged as a significant environmental concern. Both anthropogenic activities and climate change have influenced the availability and distribution of surface water resources in this area. This research endeavors to provide a comprehensive evaluation of the impacts of climate change and anthropogenic activities on surface water resources across the LUB. Various critical climatic and anthropogenic factors affecting surface water bodies, such as air temperature (AT), cropland (CL), potential evapotranspiration (PET), snow cover, precipitation, built-up areas, and groundwater salinity, were analyzed from 2000 to 2021 using the Google Earth Engine (GEE) cloud platform. The JRC-Global surface water mapping layers V1.4, with a spatial resolution of 30 m, were employed to monitor surface water patterns. Additionally, the Mann–Kendall (MK) non-parametric trend test was utilized to identify statistically significant trends in the time series data. The results reveal negative correlations of −0.56, −0.89, −0.09, −0.99, and −0.79 between AT, CL, snow cover, built-up areas, and groundwater salinity with surface water resources, respectively. Conversely, positive correlations of 0.07 and 0.12 were observed between precipitation and PET and surface water resources, respectively. Notably, the findings indicate that approximately 40% of the surface water bodies in the LUB have remained permanent over the past four decades. However, there has been a loss of around 30% of permanent water resources, transitioning into seasonal water bodies, which now account for nearly 13% of the total. The results of our research also indicate that December and January are the months with the most water presence over the LUB from 1984 to 2021. This is because these months align with winter in the LUB, during which there is no water consumption for the agriculture sector. The driest months in the study area are August, September, and October, with the presence of water almost at zero percent. These months coincide with the summer and autumn seasons in the study area. In summary, the results underscore the significant impact of human activities on surface water resources compared to climatic variables.

Keywords: climate change; anthropogenic activities; surface water resources; Google Earth Engine; Lake Urmia basin

Citation: Kazemi Garajeh, M.; Akbari, R.; Aghaei Chaleshtori, S.; Shenavaei Abbasi, M.; Tramutoli, V.; Lim, S.; Sadeqi, A. A Comprehensive Assessment of Climate Change and Anthropogenic Effects on Surface Water Resources in the Lake Urmia Basin, Iran. *Remote Sens.* **2024**, *16*, 1960. https://doi.org/10.3390/rs16111960

Academic Editor: Massimo Menenti

Received: 11 April 2024
Revised: 25 May 2024
Accepted: 27 May 2024
Published: 29 May 2024

1. Introduction

Terrestrial open-surface water bodies, such as lakes, reservoirs, ponds, streams, and rivers, play a crucial role as water resources for agriculture, industrial production, and both aquatic and terrestrial ecosystems [1–3]. Climate change and human activities have significant effects on water resources, impacting both quantity and quality [4]. Climate change can alter precipitation patterns, leading to changes in the timing, intensity, and distribution of rainfall. It can also cause glaciers to melt and snowpacks to diminish, affecting the timing and volume of water flow in rivers and streams [5,6]. Higher temperatures increase evaporation rates from surface water bodies, leading to reduced water levels in lakes, reservoirs, and rivers [7]. This can impact water availability for irrigation, hydropower generation, and ecological health [8,9]. Additionally, human activities such as deforestation, urbanization, and land-use changes can alter natural hydrological cycles, affecting water infiltration, runoff patterns, and groundwater recharge rates. These changes can impact water availability and quality, as well as the resilience of ecosystems [10,11]. Addressing the impacts of climate change and anthropogenic activities on surface water resources requires integrated strategies, including sustainable water management practices, ecosystem conservation, climate adaptation measures, and efforts to reduce greenhouse gas emissions [12].

Remote sensing technology provides an efficient means to observe the Earth's features, offering several advantages over traditional in situ measurements. Its capacity to continuously monitor the Earth's surface at various scales from regional to local makes it significantly more efficient [13]. During the last decades, remote sensing has been employed to monitor the effects of climate change and anthropogenic activities on surface water resources. Ref. [14] delved into the ramifications of climate change on water resources within the transnational Blue Nile Basin (BNB). Their study involved discerning long-term trends in hydrological time series through both parametric and nonparametric methodologies. They further refined the Soil and Water Assessment Tool (SWAT) model by calibrating it with data from various sub-basins and updated high-resolution land use and soil maps. Utilizing information from the Climate Forecast System Reanalysis (CFSR) of the National Centers for Environmental Predictions and considering three distinct climate change scenarios from the Coupled Model Intercomparison Project (CMIP3), they projected future climate change impacts. Their findings indicated a potential increase in precipitation ranging from 7% to 48%, with streamflow from the BNB potentially escalating by 21% to 97%. Similarly, ref. [15] monitored the effects of climate and land use change on forthcoming river runoff in the eastern Baltic Sea region, employing the SWAT hydrological model. They utilized the SWAT to gauge how plausible alterations in climate and land use might influence river hydrology by the century's end. Calibration of the model spanned from 1970 to 2010 (41 years) using daily river runoff data. Their results unveiled a robust linear correlation between changes in forest cover and annual river flow alterations, emphasizing the significance of land use change's impact on runoff at an annual scale. In another investigation, ref. [16] explored the impacts of climate and land use/cover change on water resources. Their study concluded that urbanization-driven land use and land cover changes contributed to over 80% of water resource fluctuations in urban areas. In contrast, climate change played a predominant role in over 55% of water resource variations in vegetated areas such as cropland, forest, and grassland. Ref. [17] explored the impacts of climate change and human activities on freshwater resources using a hydrological modeling framework. This framework integrated geographic detectors, Future Land Use Simulation (FLUS) models, and the SWAT model. It was capable of identifying the major driving factors of land use changes, predicting future land use patterns, and assessing the spatiotemporal characteristics of water resources under different future climate scenarios and land use distributions. Their findings show that the FLUS model and SWAT model can effectively simulate land use change and the runoff process with high simulation accuracy. Precipitation and temperature are identified as the main drivers of land use change. Blue

water and green water flow are more affected by climate than land use, while green water storage is more sensitive to land use change. In a recent study by [18] in the LUB, the effects of climate change and anthropogenic activities on the decline of Lake Urmia were investigated. They indicated that between 1970 and 1997, the process of change in Lake Urmia was slow; however, the shrinkage accelerated between 1998 and 2018, with approximately 30.00% of the lake area disappearing. According to their findings, anthropogenic factors had a much greater impact on Lake Urmia than climate change and prolonged drought.

A brief review of the literature reveals that these studies have typically focused on a limited set of climatic and anthropogenic variables such as precipitation, temperature, and land cover to monitor the effects of climate change and anthropogenic activities on surface water resources [19–21]. On the other hand, there are many climatic (e.g., PET) and anthropogenic (e.g., built-up area) variables that can be used to accurately monitor the effects of climate change and anthropogenic activities on surface water resources. Previous studies have also applied several hydrological methods, such as SWAT, for detecting surface water resources. However, these models are not always sufficient for detecting various types of surface water resources, such as seasonal ones. Additionally, they can sometimes be time-consuming since they need to be applied separately for each time interval if the temporal scale is long. In recent years, Google Earth Engine (GEE), a cloud-based geospatial analysis platform, has been employed to monitor the effects of climate change and anthropogenic activities on the Earth's features [22–29]. The integration of the GEE platform has significantly enhanced research accessibility, offering robust computational resources at no cost [25,30]. GEE finds extensive application in monitoring Earth's features on a large scale and over extended periods. Furthermore, the platform boasts an extensive array of datasets, including Moderate Resolution Imaging Spectroradiometer (MODIS) products (e.g., MOD21A1D.061), Landsat (e.g., JRC Global Surface Water Mapping Layers), Global Precipitation Measurement, etc., which allows for simplifying data acquisition and enabling collaborative analysis across various datasets to enhance algorithm accuracy [31,32]. In the realm of monitoring climate change and the impact of human activities on surface water resources, accurate information regarding these resources, as well as climatic and anthropogenic variables, is of paramount importance [33]. Global datasets detailing the location and seasonal fluctuations of surface water have been compiled using inventories, national reports, statistical extrapolation from regional data, and satellite imagery. Nonetheless, achieving precise measurements of long-term changes at a high resolution remains a formidable challenge [33,34]. While remote sensing methods and products have been utilized for mapping surface water resources in research (e.g., MODIS land water mask products), it is crucial to incorporate newer products such as the JRC Global Surface Water Mapping Layers, which boasts a spatial resolution of 30 m, to enhance these datasets and methodologies [35]. This product provides valuable insights into the extent and changes in surface water resources, offering comprehensive statistics on seasonal, temporal, monthly, and permanent reservoir information [35,36]. It sets itself apart from other datasets, including the Global Land Analysis and Discovery (GLAD) dataset [37] spanning from 1999 to 2020, the Global Surface Water Dataset (GSWD) [35] covering 1984 to 2015, and the Landsat Dynamic Surface Water Extent (DSWE) dataset developed by [38].

As mentioned, previous studies have considered a small number of climatic and anthropogenic variables for monitoring their effects on the Earth's features. Previous research has also employed several hydrological models and MODIS land water mask products with a spatial resolution of 250 m for detecting patterns in surface water resources. Building on the review of the previous literature, this study addresses the limitations of past research by (1) broadening the scope by incorporating a diverse range of climatic and anthropogenic variables, including air temperature (AT), cropland (CL), potential evapotranspiration (PET), snow cover, precipitation, built-up area, and groundwater salinity, to better understand their patterns and effects climate change and anthropogenic activities on surface water resources; (2) utilizing high-resolution data by employing Landsat-based data, specifically the JRC Global Surface Water Mapping Layers v1.4 at a spatial resolution of 30 m, to monitor the variation in various surface water resources; and (3) assessing the relationships between predisposing variables and surface water resources using the Mann–Kendall (MK) non-parametric trend test.

2. Study Area

The Lake Urmia Basin (LUB) is a significant geographical and ecological region situated in northwestern Iran, encompassing an expanse of 51,876 km^2 (as depicted in Figure 1). At its heart lies Lake Urmia, once renowned as one of the largest saltwater lakes in the Middle East. Lake Urmia has held historical significance for its ecological importance and its support of local communities through human activities like agriculture, fishing, and tourism [39]. However, its size has drastically diminished in recent decades due to a multitude of factors, including river damming, excessive water usage for agriculture, and droughts induced by climate change [40]. The LUB is sustained by a network of 60 rivers, including 21 permanent or seasonal and 39 intermittent streams. Noteworthy among these are the Zarineh, Simineh, and Aji Chai rivers, serving as the primary inflows to Lake Urmia [41]. Within the basin, various surface water sources, including seasonal rivers, intermittent streams, internal springs, as well as rainfall and snowfall, contribute to sustaining Lake Urmia. The rivers within this watershed exhibit distinct characteristics, with those originating from high-altitude sources such as Sahand, Savalan (Sabalan), and Chehel Cheshme in Kurdistan flowing relatively longer distances and remaining perennial. Examples include Aji Chai, Zarineh River, Simineh River, and Sufi Chai. In contrast, rivers to the west, southwest, and north of the lake, which have shorter courses and lower water volumes, include Godar Chai, Nazlo Chai, and Zola Chai [42]. The region experiences a semi-arid and dry/cold climate, with an average annual rainfall of 359 mm, minimum temperatures of 4.3 °C, and maximum temperatures of 17.7 °C. Evaporation rates range from 930 to 1513 mm per year. Approximately 25% of the lake's inflow comes from direct precipitation, with the remaining 75% sourced from the network of rivers [43]. The diminishing size of Lake Urmia is causing severe environmental and socio-economic ramifications, such as increased salinity levels, habitat loss for migratory birds, and the displacement of local communities reliant on the lake. Various endeavors, including water management initiatives, restoration projects, and international collaborations, have been initiated to address these challenges. Nevertheless, restoring the lake to its former splendor remains a multifaceted and arduous endeavor necessitating sustained efforts from diverse stakeholders [44].

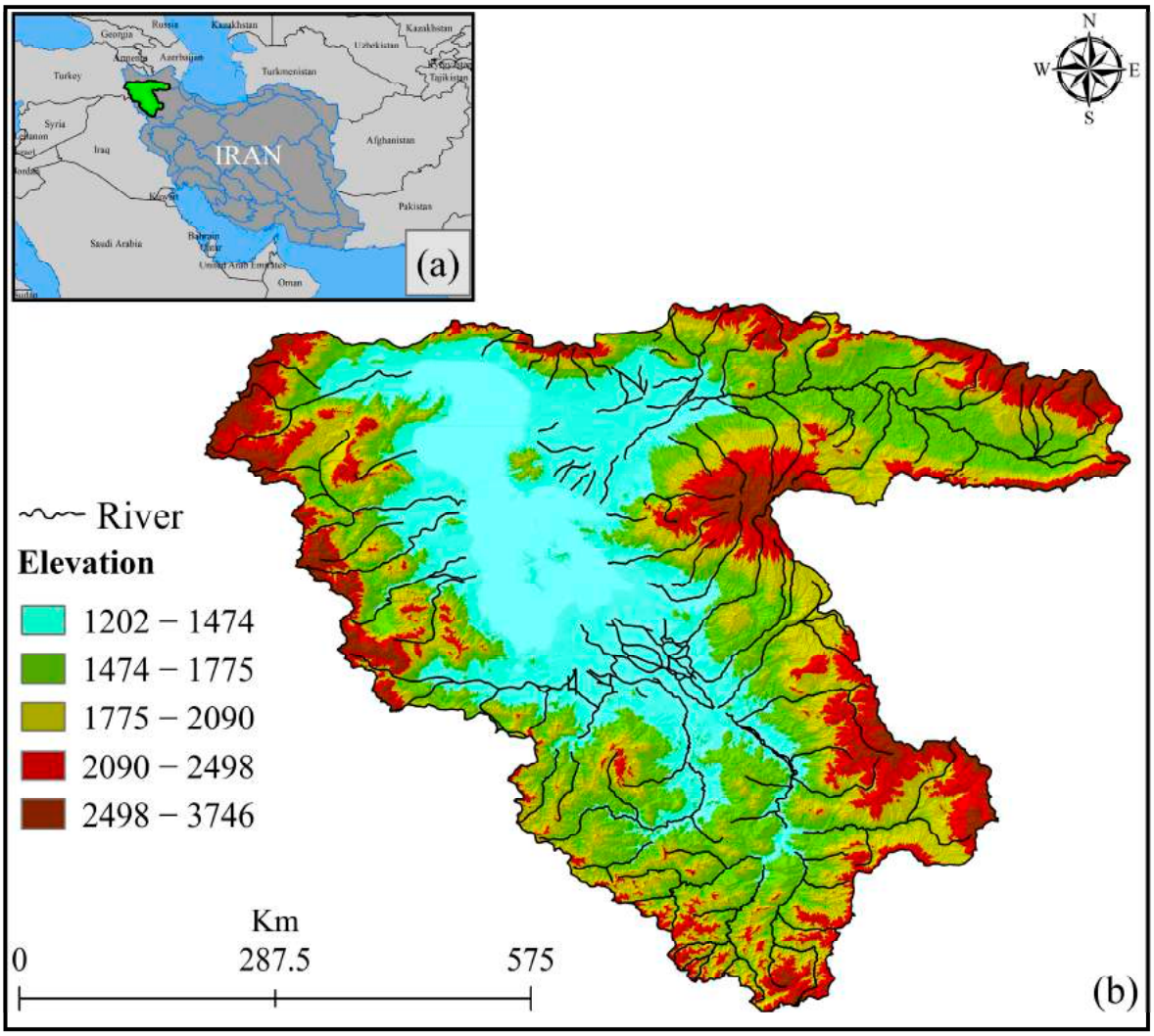

Figure 1. Location of the study area in (**a**) Iran basins and (**b**) ULB.

3. Methodology

We employed various remote sensing datasets on the GEE platform to monitor the effects of climate change and anthropogenic activities on surface water resources. These datasets cover the period 2000 to 2021 and include climatic and anthropogenic variables (Figure 2) such as AT, CL, PET, snow cover, precipitation, built-up area, and groundwater salinity, which were employed in this study (details in Table 1). This study also utilized Landsat series images (Landsat 5, 7, and 8) to check the variation in various surface water resources (e.g., seasonal rivers, dams). Additionally, the JRC Global Surface Water Mapping Layers v1.4 was used to monitor the variation in surface water resources over the study area from 1984 to 2021. The variations in surface water resources across different categories (permanent, seasonal, lakes) are presented in Figure 3. Additionally, Figure 4 depicts the trends in surface water resources for each month from 1984 to 2021.

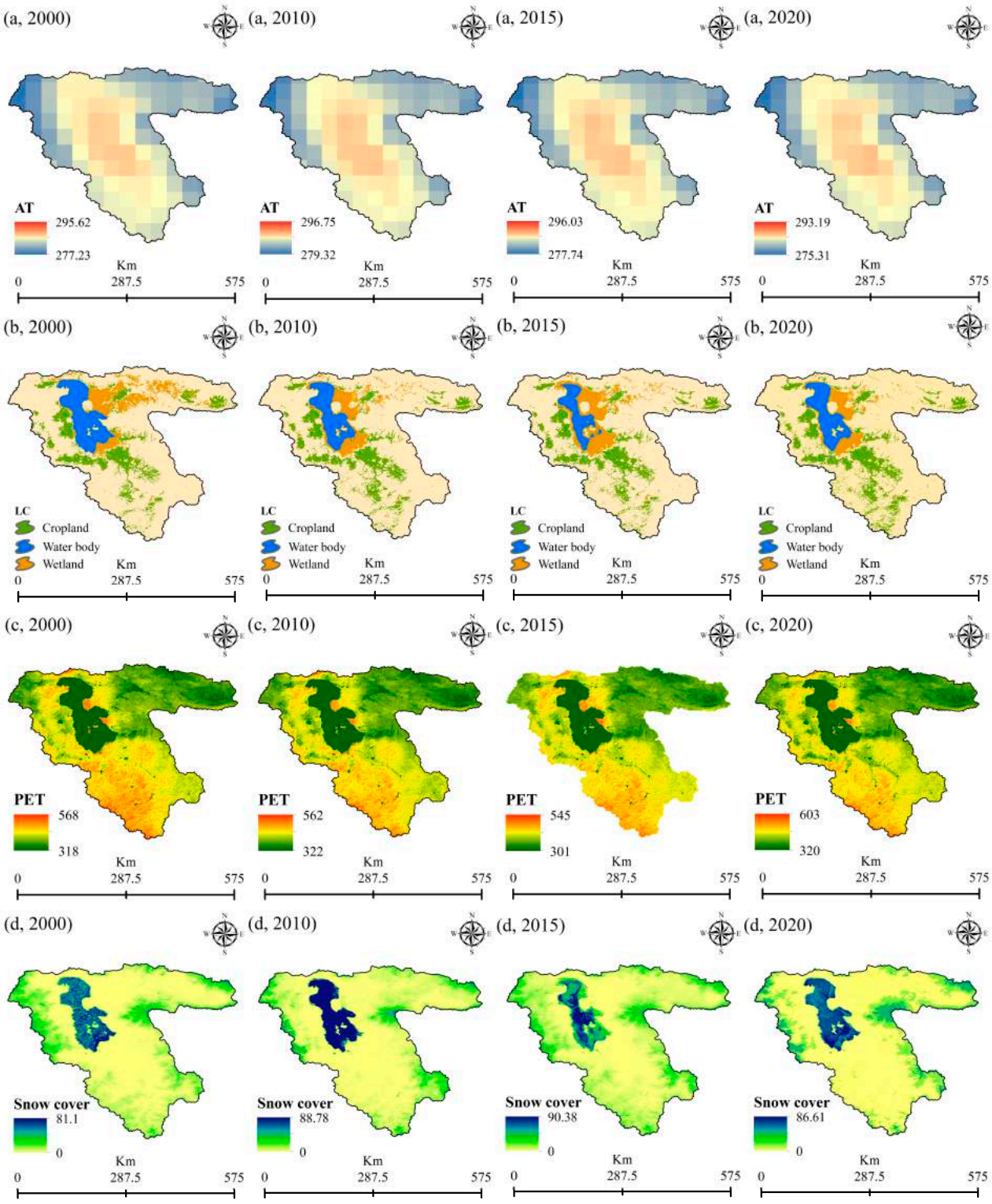

Figure 2. *Cont*.

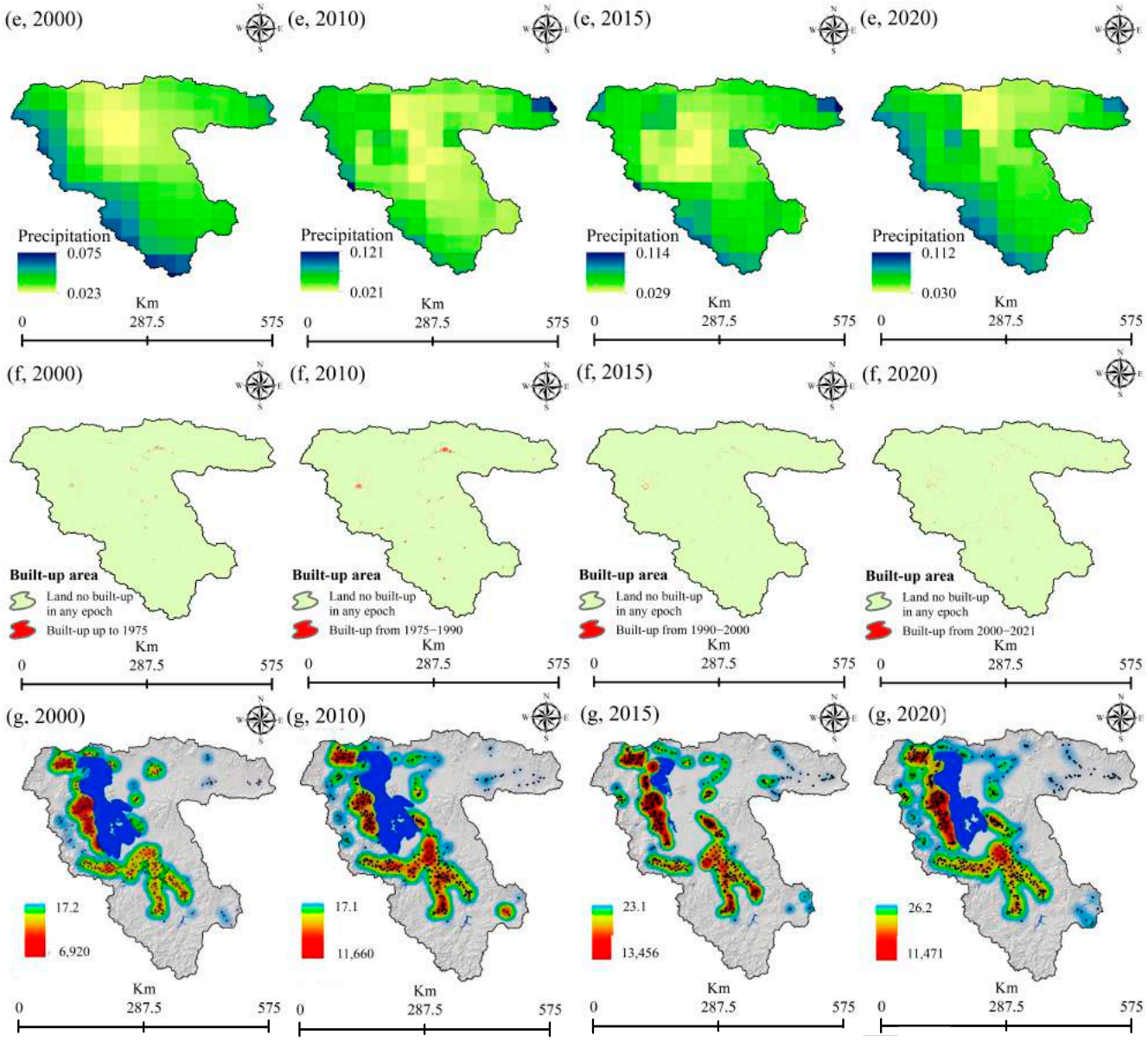

Figure 2. Various predisposing variables for monitoring climate change and anthropogenic effects on surface water resources, including: (**a**) AT for the years 2000, 2010, 2015, and 2020; (**b**) LC for the years 2000, 2010, 2015, and 2020; (**c**) PET for the years 2000, 2010, 2015, and 2020; (**d**) snow cover for the years 2000, 2010, 2015, and 2020; (**e**) precipitation for the years 2000, 2010, 2015, and 2020; (**f**) built-up area for the years 2000, 2010, 2015, and 2020; and (**g**) groundwater salinity for the years 2000, 2010, 2015, and 2020.

Table 1. Characteristics of various climatic and anthropogenic variables for monitoring climate change and anthropogenic effects on surface water resources.

Variable	Spatial Resolution	Temporal Resolution	Product's Name	Unit	References
Air temperature	11 km	Daily (1979–2024)	ERA5-Land	K	[45]
Cropland	500 m	Yearly (2000–2024)	MCD12Q1	Sq.km	https://doi.org/10.5067/MODIS/MCD12Q1.061 (accessed on 2 March 2024)
Potential evapo-transpiration	500 m	8-day composite (2000–2024)	MOD16A2GF.061	$Kg/m^2/day$	[46]
Snow cover	500 m	Daily (2000–2024)	MOD10A1.061	%	[47]
Precipitation	28 km	Monthly (1998–2024)	TRMM 3B43: Monthly Precipitation Estimates	Mm/hr	[48]
Built-up area	100 m	5 year intervals (1975–2030)	GHSL: Global built-up surface	Meter	[49]
Groundwater salinity	100 m	Annually (2000–2021)	Water quality index	Electrical conductivity (EC)	[50]

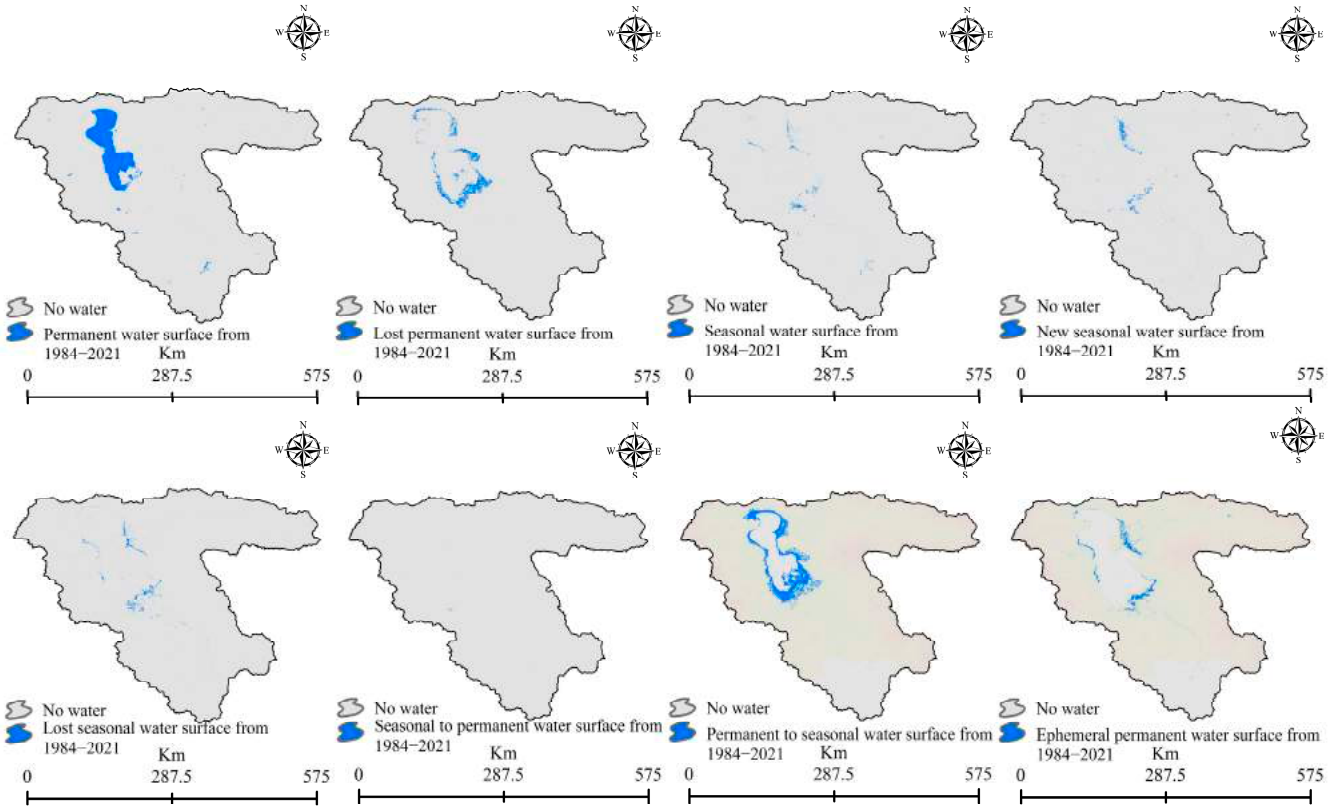

Figure 3. Changes observed in various surface water resources from 1984 to 2021 depicted in the JRC Global Surface Water Mapping Layers, version 1.4.

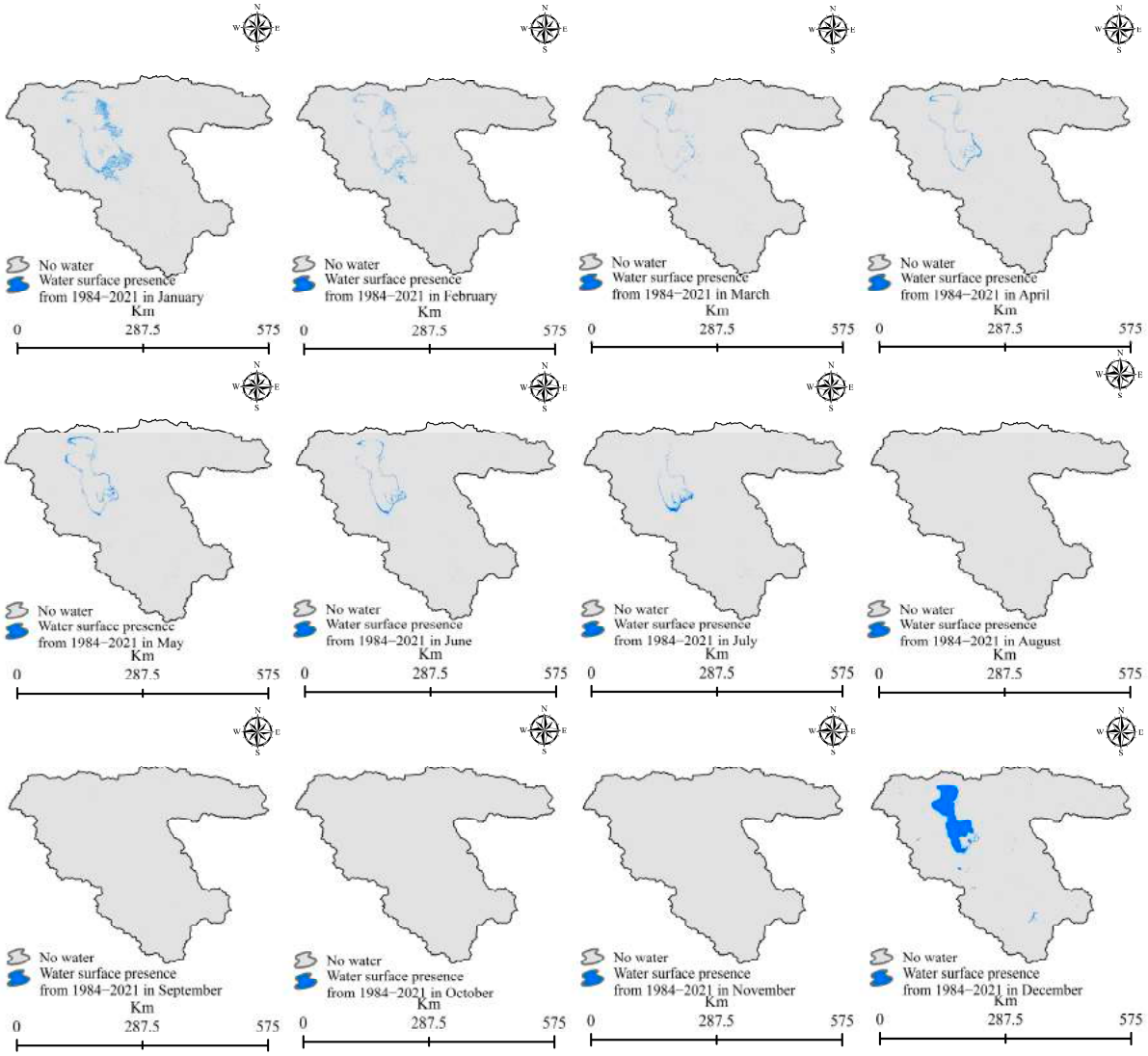

Figure 4. Changes observed in various surface water resources in different months from 1984 to 2021 depicted in the JRC Global Surface Water Mapping Layers, version 1.4.

The methodology used in this study is represented in Figure 5. A typical workflow for preprocessing remote sensing products in GEE includes data acquisition, region of interest selection, temporal filtering, targeted feature extraction, and data export. In this study, various climatic, anthropogenic, and surface water products listed in Table 1 were identified and imported using the implemented code (https://code.earthengine.google.com/13783dee2b7480daa0ad69c861a247b9 (accessed on 2 March 2024)). GEE variables encompass a range of data types such as images, geometries, feature collections, numbers, strings, and more. Given that our data type (for calling climatic, anthropogenic and surface water datasets available in the GEE) is an image, we opted for this to align with our analysis or visualization needs. The region of interest for analysis was then defined, which can either be predefined administrative boundaries or other predefined regions such as countries or continents. The region of interest is represented using geometries, which can be points, lines, polygons, or collections of such geometries. This will restrict the image to only include the pixels within the defined polygon region of interest, which is the LUB prepared in the ArcGIS 10.8 environment. After specifying study period (2000–2021), several variables, including AT, LC, PET, snow cover, precipitation, and built-up area were extracted from ERA5-Land, MCD12Q1, MOD16A2GF.061, MOD10A1.061, TRMM 3B43: Monthly Precipitation Estimates, and JRC/GHSL/P2016/BUILT_LDSMT_GLOBE_V1 products, respectively,

which are freely available in GEE like in JRC. In addition to defining a time series chart for each variable separately, we extracted climatic and anthropogenic variables and exported them to the ArcGIS 10.8 environment to visualize the variation in employed factors. This allows for monitoring the effects of climate change and anthropogenic variables on surface water resources. Exporting could be performed in various formats such as GeoTIFF, CSV, or directly to Google Drive [51]. To analyze the variation in various variables, datasets were extracted in both GeoTIFF and CSV formats. ArcGIS 10.8 was utilized for mapping and estimating the areas of variables from 2000 to 2021, as illustrated in Figures 2–4. Microsoft Excel was employed for designing graphs and estimating correlation coefficients between variables and surface water resources.

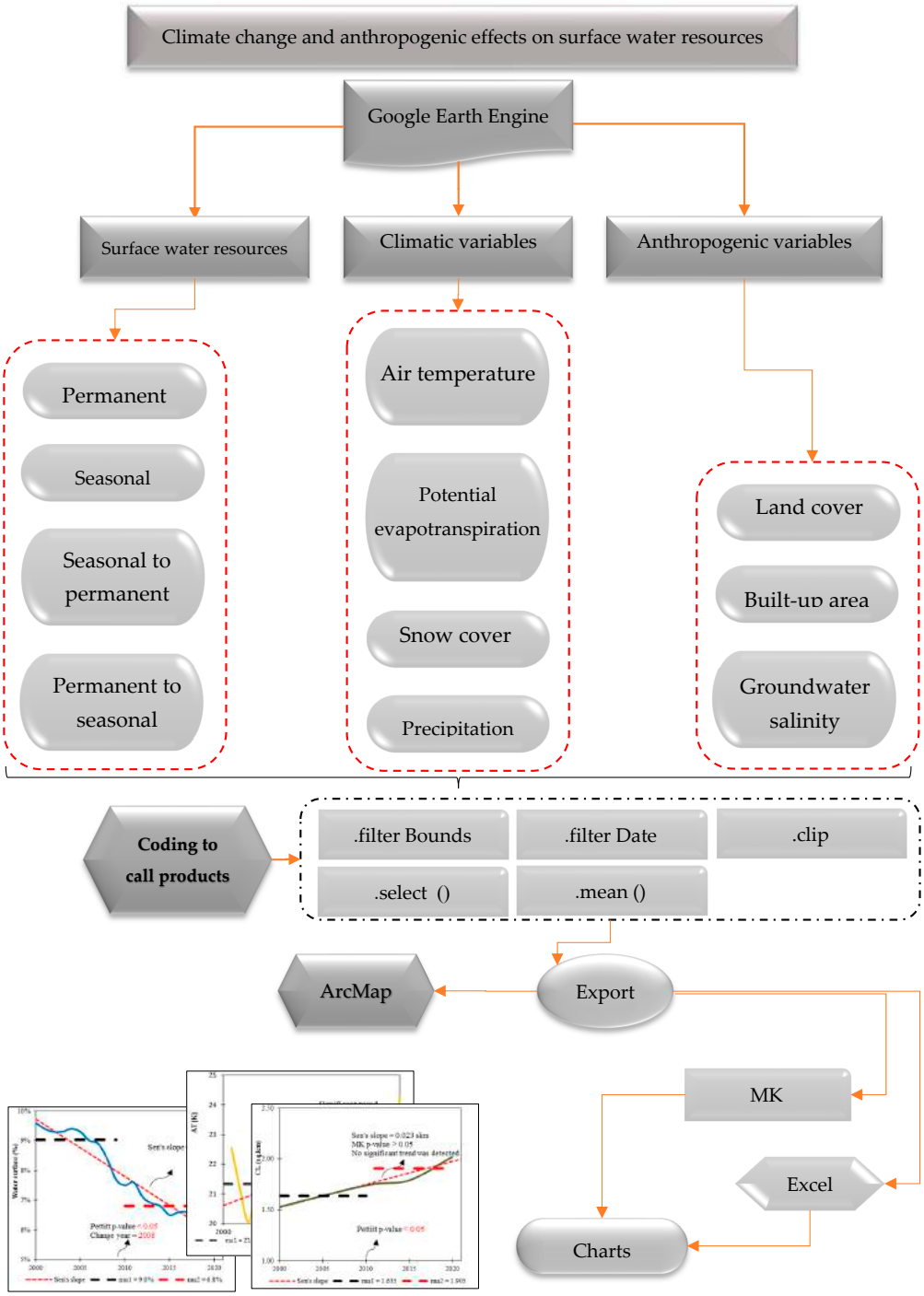

Figure 5. An overview of the applied methodology.

The Mann–Kendall (MK) non-parametric trend test is commonly used to identify statistically significant trends in time series data [52]. To address the issue of serial correlation effect, a modified version of the MK test was utilized. This modification likely adjusts for any autocorrelation present in the data, ensuring the robustness of the trend analysis results. Additionally, Pearson correlation analysis was conducted. The Pearson correlation analysis is useful for assessing the strength and direction of relationships between variables while controlling for the effects of other variables [53]. The Mann–Kendall test and Pearson correlation analysis have been extensively used in previous studies worldwide to investigate climate variability and its impacts on surface water resources, as exemplified by [54]. Overall, these methodologies provide robust tools for analyzing temporal trends and relationships between climate factors and surface water resource dynamics, thereby contributing to a better understanding of climate change impacts on hydrological systems. For further information, please refer to [55,56].

4. Results

4.1. Analysis of the Relationship between Surface Water Resources and Various Climatic and Anthropogenic Variables

Figures 6 and 7 illustrate the significant relationships between climate change, anthropogenic activities, and surface water resources across the LUB from 2000 to 2021. Figure 6 highlights a significant relationship between climate change and the effects of anthropogenic activities on surface water resources across the LUB from 2000 to 2021. The negative correlation coefficient of −0.56 between surface water resources and AT, as indicated in Figures 6 and 7, aligns with the findings of [57], showing a warming trend of approximately 0.18 °C per decade over recent decades. Lake Urmia, the primary surface water source in the LUB, began to experience drying trends from the year 2000 onwards. As temperatures rose, the lake's influence on the local climate intensified, particularly during summer months, with winter seeing comparatively lesser effects. While the declining lake level has indeed affected local climate conditions, its impact has been somewhat mitigated. Regarding anthropogenic effects on surface water resources, an increase in built-up areas corresponds to higher water consumption due to population growth. Figure 6 reveals a strong negative correlation coefficient of −0.99 between the built-up area and surface water resources. The accelerated expansion of built-up areas and the burgeoning population exert added strain on surface water reserves [58]. In the period spanning from 1976 to 2010, the populace within the Lake Urmia Basin surged by 121.5% [59]. A positive correlation coefficient of 0.12 between surface water resources and PET is reflected in Figure 6. The correlation between precipitation and PET is clear: a decrease in precipitation directly impacts PET, reducing its value. The authors of [60] also noted a significant increase in agricultural and urban lands between 1987 and 2016, consistent with our findings, which show a correlation coefficient of −0.89 between cropland and surface water resources. The study concludes that the expansion of the total irrigated area has led to a heightened demand for water for irrigation throughout the study period. Moreover, Figure 6 indicates a positive correlation coefficient between precipitation and surface water resources, suggesting that decreased precipitation leads to a reduction in surface water area, which is opposite by the findings of [40]. In terms of snow cover, a correlation coefficient of −0.09 was found between snow cover and surface water resources. The recent drought has impacted the snow cover over the LUB, as demonstrated by [61]. They demonstrate significant interannual variability in the snow cover, yet the annual trends for both the snow cover and snow line elevation were found to be non-significant. Lastly, a correlation coefficient of −0.79 was estimated between groundwater salinity and surface water resources, in line with the findings of [50].

Variables	Surface water	AT	Built-up area	PET	CL	Precipitation	Snow cover	Groundwater salinity
Surface water	1	−0.56	−0.99	0.12	−0.89	0.07	−0.09	−0.79
AT	−0.56	1	−0.71	0.58	−1.00	−0.36	−0.60	−0.82
Built-up area	−0.99	−0.71	1	−1.00	0.88	0.50	0.70	0.71
PET	0.12	0.58	−1.00	1	−1.00	−0.48	−0.18	−1.00
CL	−0.89	−1.00	0.88	−1.00	1	0.50	0.90	0.87
Precipitation	0.07	−0.36	0.50	−0.48	0.50	1	0.18	0.99
Snow cover	−0.09	−0.60	0.70	−0.18	0.90	0.18	1	0.99
Groundwater salinity	−0.79	−0.82	0.71	−1.00	0.87	0.99	0.99	1

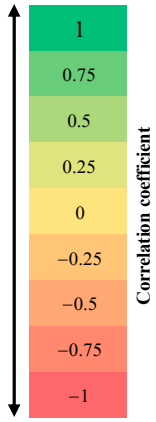

Figure 6. Correlation between different climatic and anthropogenic variables and surface water resources across the LUB, analyzed using the Pearson correlation heatmap.

This study reveals significant trends in various climatic and anthropogenic variables over the past two decades in the LUB region, as indicated in Figure 7. Surface water areas experienced a notable decline of 2.0% decade-1 ($p < 0.05$), with a marked downward shift in 2008. Before the shift, the average sub-series was 9%, which decreased to 6.8% after the shift. Additionally, AT exhibited a significant increase of 1.02 °C decade-1, with a noticeable upward shift in 2012, leading to a post-shift average sub-series 1.2 °C higher than pre-shift levels (Figure 7). CL in the LUB displayed a significant increase of 0.023 sq.km decade-1 ($p < 0.05$), accompanied by an upward abrupt shift, as indicated in Figure 7. Before the shift, the average sub-series was 1.63 sq.km, increasing to 1.90 sq.km after the shift. Conversely, PET witnessed a significant decline of −4254 mm/d decade-1, marked by a downward shift in 2010. The pre-shift average sub-series was 476,758 mm/d, decreasing to 422,179 mm/d post-shift, as shown in Figure 7. Regarding snow cover and precipitation, there was a non-significant increase of 0.36% decade-1 and 0.0022 mm/hr decade-1, respectively. According to Figure 7, built-up areas in the LUB experienced a significant increase of 0.00006 sq.km decade-1 ($p < 0.05$), with an upward abrupt shift. The average sub-series rose from 0.0825 sq.km before the shift to 0.0833 sq.km after the shift. Moreover, groundwater salinity exhibited a significant increase of 0.535 EC decade-1 ($p < 0.05$), accompanied by an upward abrupt shift. The average sub-series increased from 17.150 EC before the shift to 24.650 EC after the shift, as indicated by Figure 7.

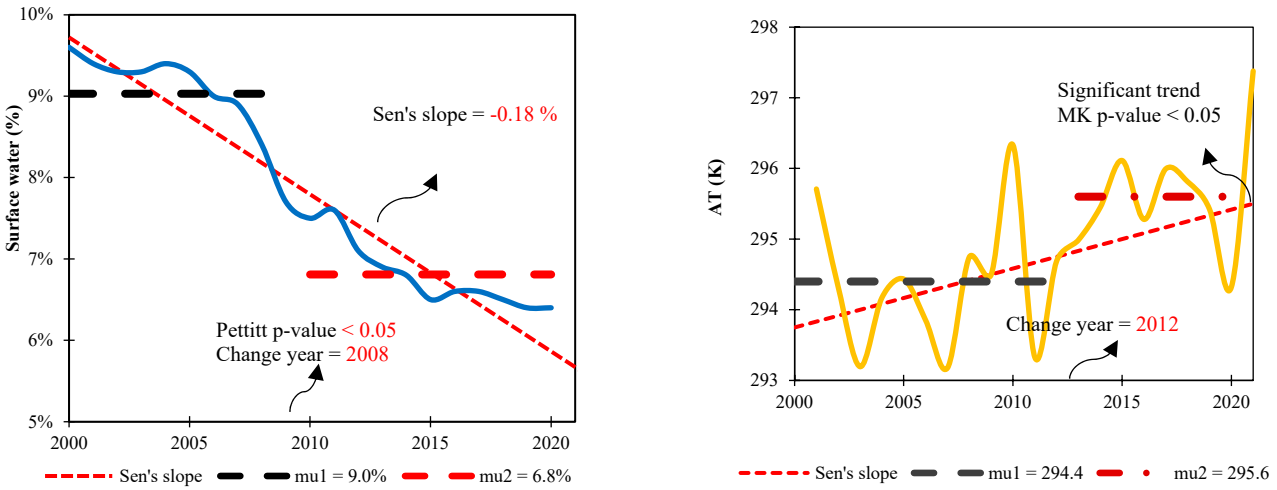

Figure 7. *Cont.*

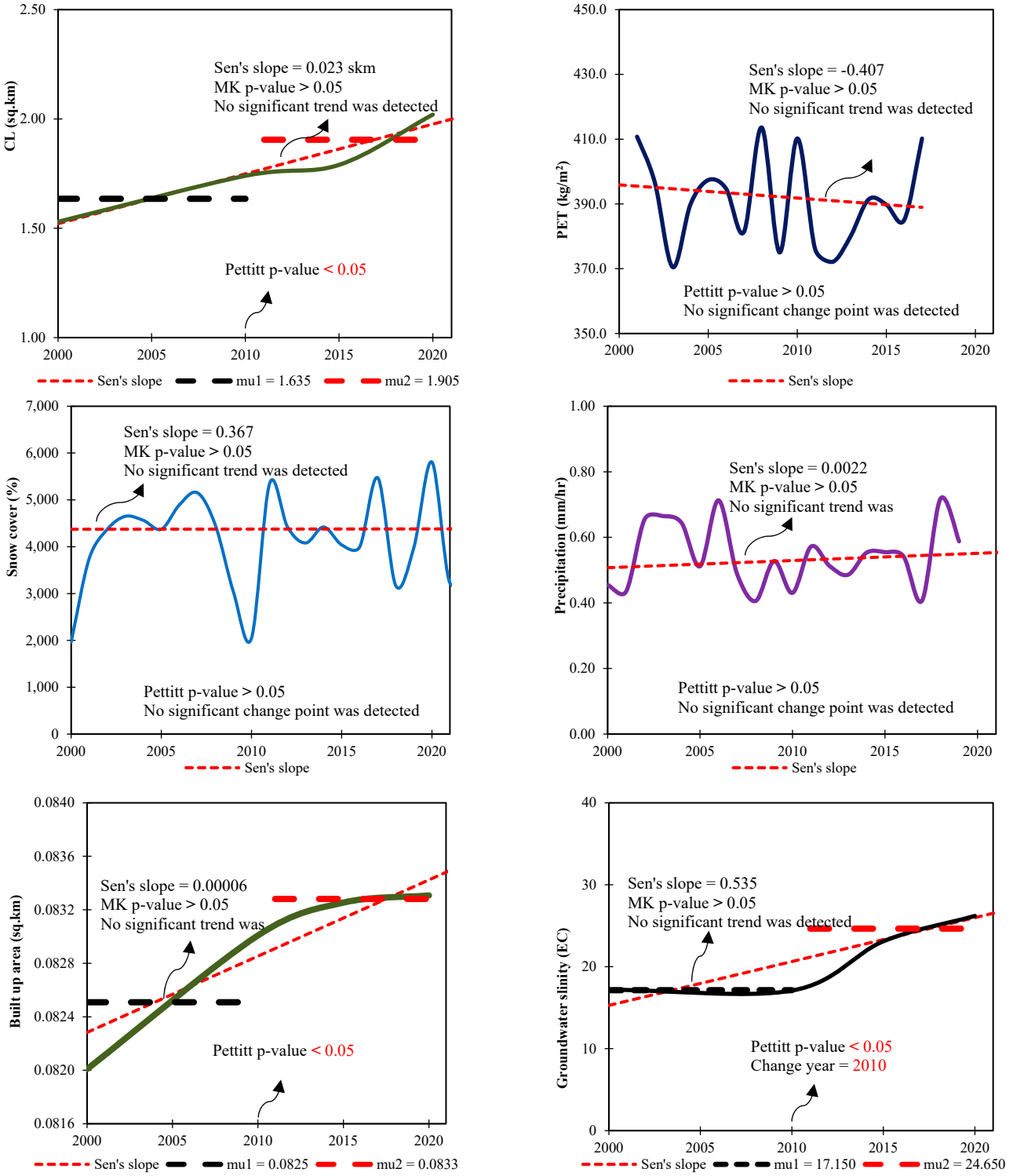

Figure 7. Time series analysis depicting the annual variations and trends in surface water bodies and climatic and anthropogenic variables, including AT, CL, PET, snow cover, precipitation, built-up areas, and groundwater salinity, throughout the LUB. The significance of the trend lines was determined using the Mann–Kendall test. The trend line slope is based on Sen's slope estimator. In cases where a time series experienced a significant abrupt shift, identified by Buishand's test, the change year is indicated. For these instances, "mu" denotes the average of the sub-series.

4.2. Analysis of the Various Surface Water Resources Variation from 1984 to 2021

Figures 8 and 9 illustrate changes in surface water resources across the LUB from 1984 to 2021. Notably, 38.65% of the area has remained consistently water covered throughout this period, classified as permanent water. However, permanent water resources have also experienced a net loss of 12.78%, with a small gain of 0.34% in newly designated permanent water areas. The analysis also reveals seasonal water resources, with 2.74% of the LUB identified as such. While there has been a net gain of 0.38% in seasonal water resources, a concerning trend is the conversion of 28.99% of permanent water to seasonal water over the study period (Figure 9). Notably, no transitions from seasonal to permanent water were observed. Furthermore, Figure 9 shows that 0.48% and 7.84% of the surface water resources have been classified as ephemeral permanent and ephemeral seasonal, respectively. These classifications likely represent short-term fluctuations in water presence. Consistent with the LUB's climate, December and January exhibit the highest presence of water (Figure 9), coinciding with winter months when agricultural water consumption is minimal. Conversely, August, September, and October, corresponding to summer and autumn, are the driest months, with minimal water presence.

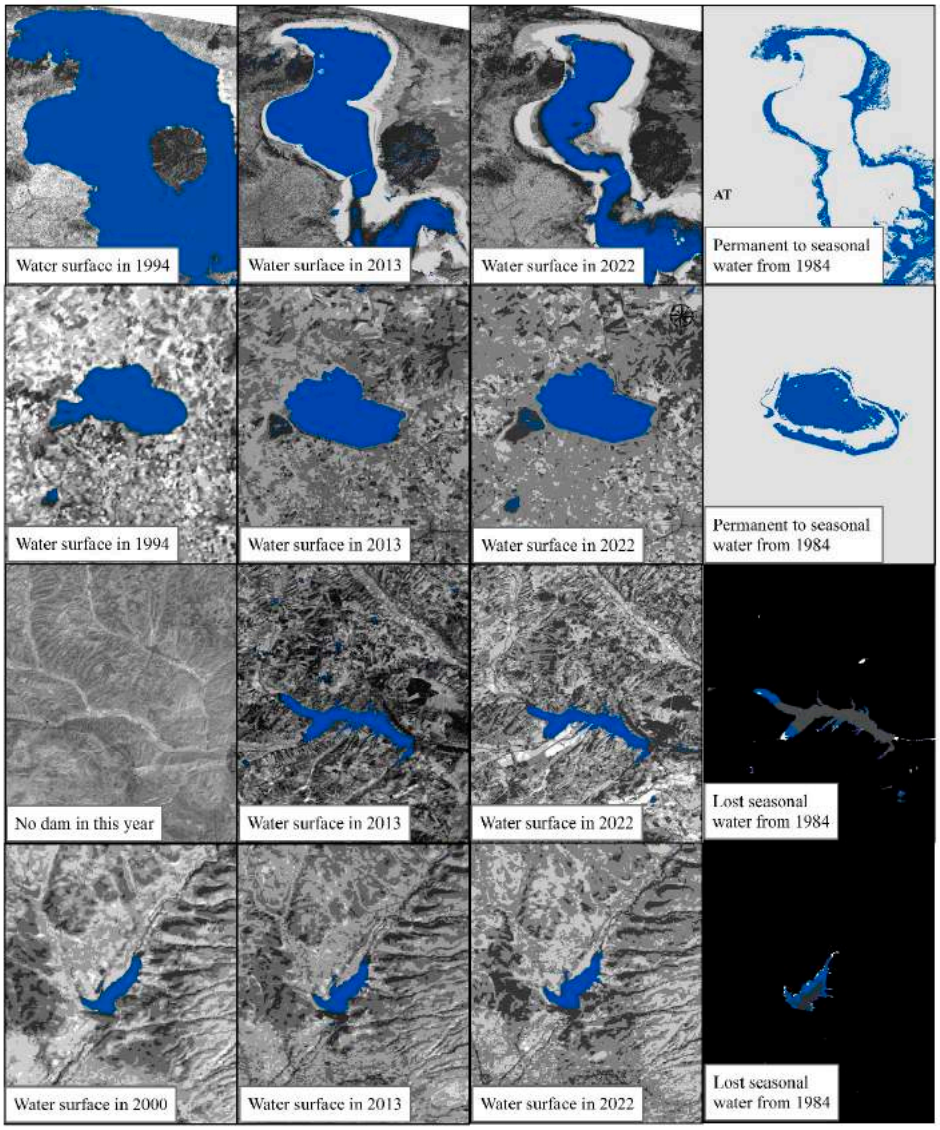

Figure 8. Surface water changes in various surface water resources from 1984 and 2000 to 2022 obtained from Landsat 5, 7, and 8 series images.

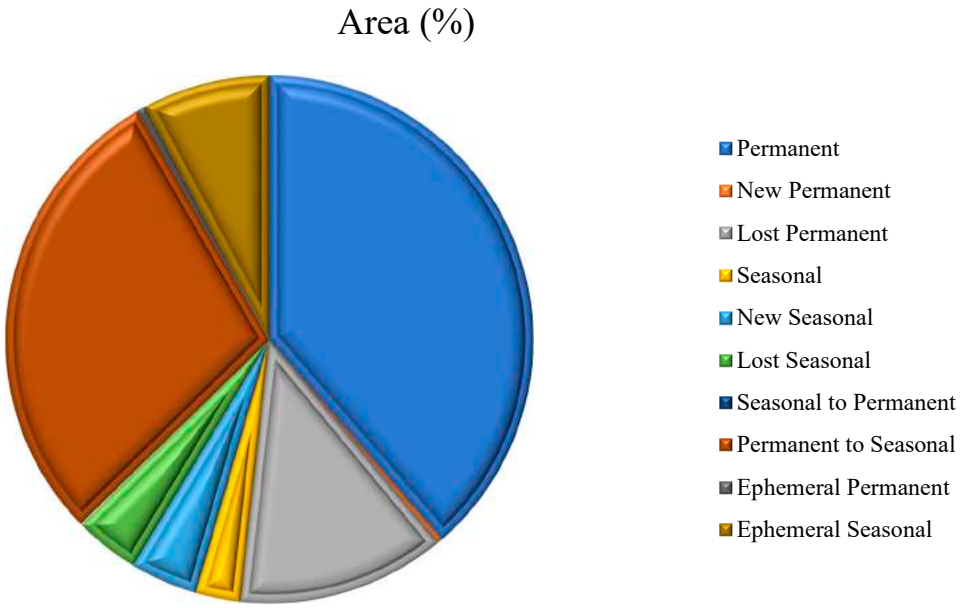

Figure 9. Changes in surface water body transitions from 1984 to 2021 in the LUB [62].

5. Discussion

5.1. General Discussion

This research quantified the impact of both climate change and human activities on surface water resources in the LUB from 2000 to 2021. Our findings reveal significant associations between various climatic and human-induced factors and the decline in surface water resources. While previous studies [19–21] typically concentrated on a limited set of variables like precipitation, temperature, and land cover, our study aims to expand this scope by incorporating a diverse range of factors such as AT, CL, PET, snow cover, precipitation, built-up area, and groundwater salinity. This broader approach offers a deeper understanding of the influences of climate change and human actions on surface water storage. Additionally, our study utilizes Landsat-based data, specifically the JRC Global Surface Water Mapping Layers v1.4, which provide detailed information on various surface water resources like permanent and seasonal rivers at a spatial resolution of 30 m, enhancing the accuracy and detail of our analysis. Our results underscore the significant impact of human activities on surface water resources compared to climatic variables. Anthropogenic factors such as built-up area, CL, and groundwater salinity exhibit strong negative correlations (-0.99, -0.89, and -0.79, respectively) with surface water resources. This study reveals that mismanagement of surface water resources, expansion of agricultural farmlands, and overuse of aquifers have led to a drought in the lake, extensive land degradation, and heightened salinity levels, posing serious threats to the population. Over the past three decades, inadequate sustainable development strategies and mishandling of the fragile ecosystem have exacerbated these issues. The scarcity of water in the LUB region has triggered various ecological problems. Studies indicate a 90% decline in the Artemia population due to the lake's shrinkage. Moreover, salinity levels have surged in recent years, saturating the lake water with salts and causing salt crystals to form on its surface year-round [62]. The diminishing surface water resources in the LUB have caused a decline in vegetation, resulting in a significant rise in the frequency and severity of dust storms in the area. These storms adversely affect over 7 million residents, posing health risks and socioeconomic challenges, reducing soil fertility in agriculture, and weakening vegetation. Furthermore, recurring declines in water availability could jeopardize food security in the region, given that agriculture in the LUB serves as a primary food source, making water scarcity a substantial threat to this sector [63,64]. However, the implementation of practical methodologies could greatly assist decision-makers in water management. By enabling them to anticipate and simulate the impacts of climate change and human activities on

surface water resources, such approaches could help mitigate the challenges faced by the region.

5.2. Analysis of the Effects of Anthropogenic Variables on Surface Water Resources

The LUB is sustained by a network of 60 rivers, including 21 permanent or seasonal and 39 intermittent ones. Notably, the Zarineh and Simineh Rivers and Aji Chai are primary inflows to Lake Urmia [65]. Over the past decade, several new dams and irrigation districts have been developed in the basin, leading to increased consumptive use of tributary river waters. As of 2012, there are over two hundred approved new dams and irrigation projects either under construction or in the final design stages [66]. Despite no significant trend in the drought pattern, the observed physiographic changes in Lake Urmia may be attributed to dam construction, irrigation projects, and overuse of surface water and groundwater [67]. High agricultural water demand due to low irrigation efficiency, cultivation of water-intensive crops, and extensive agriculture exacerbate this environmental crisis. The authors of [68] introduced a novel method for designing environmental flow to Lake Urmia, highlighting the mismanagement of water consumption in the agricultural sector of the LUB, resulting in an 80% decline in inflow to the lake. Between 2010 and 2015, the combined water consumption and renewable water sources surpassed 4.83 × 109 and 7.00 × 109 m^3, respectively. However, agricultural water use accounted for 4.30 × 109 m^3. The agricultural sector's water consumption constituted approximately 65% of the total renewable water sources and 93% of the overall water use in the LUB [69]. Yet, it is noted that the acceptable withdrawals from renewable water sources should ideally fall within the range of 20% to 40% of total water consumption. Moreover, from 1986 to 2013, water-based farmland in the basin expanded from 3.50 × 105 to 5.00 × 105 hm^2. The substantial water consumption in the agricultural sector within the basin has led to a sharp decline in the lake's water volume (SPSS CC = –0.77). Thus, it is imperative to devise strategic plans to curtail water usage in agriculture to stabilize the lake's volume. The shrinking of Lake Urmia starkly demonstrates that the natural supply capacity of water resources in the LUB is insufficient to meet the rapidly increasing water demand. Regarding anthropogenic effects, increasing domestic water consumption and population growth in the LUB have escalated total water demand [70]. According to data from the Agricultural Statistics and Information Center of the Ministry of Agriculture of Iran, the population of the LUB was 1.86 × 106 and 5.48 × 106 in 1970 and 2020, respectively. There exists an inverse relationship between population growth and the total volume of water in Lake Urmia (SPSS CC = −0.71).

The analysis of anthropogenic variables reveals a significant increase in built-up areas within the LUB region from 2000 to 2020, as shown in Figure 2. This expansion of urban areas is in accordance with population growth, consequently driving higher water consumption demands. With growing populations comes an increased need for food production, leading to heightened irrigation requirements for agricultural lands [71,72]. Our findings further demonstrate a noticeable rise in cropland coverage across the LUB during the same period, primarily driven by the escalating demand for food to support the growing populace. The proportion of water utilized in crop cultivation is influenced by various factors, notably the type of irrigation technology employed. Given that traditional irrigation methods predominate in the LUB, there is a considerable reliance on surface water resources. Concerning groundwater salinity, our study reveals a concerning trend of water resource salinization within the study area from 2000 to 2020. Notably, the agricultural sector stands out as the primary consumer of water resources in the LUB [73], with approximately 73 thousand wells situated around Lake Urmia. These wells have witnessed an upward trend in water extraction in recent years, exacerbating concerns over groundwater depletion.

5.3. Analysis of the Effects of Climatic Variables on Surface Water Resources

As emphasized, the impact of anthropogenic variables on the reduction in surface water is significant. However, it is equally important to acknowledge the effects of climate

change on surface water resources across the study area, akin to anthropogenic factors. Climatic factors such as AT, PET, precipitation, and snow cover demonstrate negative correlations of −0.56 and −0.09 for AT and snow cover with surface water resources. Additionally, they show positive correlations of 0.12 and 0.07 for PET and precipitation with surface water resources. Ref. [60] demonstrated a time series correlation between precipitation across the entire basin and variations in Lake Urmia's water level. They noted that for the entire modeling period, the correlation of annual changes in lake levels with precipitation and temperature stands at 0.15 and −0.36, respectively. However, after 1995, the lake level displays a relatively weak correlation of −0.12 with precipitation. Despite notable increases in precipitation in 2003 and 2006, the lake level continues to plummet abruptly. Conversely, the correlation between temperature and lake level reaches from 0.15 to −0.28 during the period from 1995 to 2010. With the observed rise in temperature after 1995, it is expected that higher rates of evaporation over the lake would occur. However, there is a positive correlation coefficient of 0.15 between PET and surface water resources, suggesting that a reduction in water volume would decrease the potential for evaporation. Within the realm of snow cover, a correlation coefficient of −0.09 is noted between snow cover and surface water resources. Ref. [61] indicates significant inter-annual variability in snow cover, with non-significant annual trends observed for both snow cover and snow line elevation. Furthermore, no significant trend is identified for snow depletion curve indices. The study underscores the greater significance of evaporation and atmospheric evaporative demand in reducing snow cover compared to the role of precipitation in increasing snow cover.

In the domain of climatic variables' effects on surface water resources, this study shows an increase of 0.41 °C in AT from 2000 to 2015, as can be seen in Figure 2. An increase in AT would increase surface water evaporation and water consumption. Among other climatic variables, our findings indicate an increase in PET from 2000 to 2020 over the study area, as shown in Figure 2. PET incorporates the idea of consumptive usage, acknowledging a large amount of water that cannot be reused or recovered, and instead considers plant consumption of water that evaporates. The results of this study show that PET decreased from 2000 to 2015, since surface water resources, especially Lake Urmia, have declined significantly during this period. In 2020, on the other hand, the rate of PET increased, as can be seen in Figure 2. In terms of precipitation, there is an increase from 2000 to 2010 over the study area. However, from 2010 to 2020, the precipitation rate decreased in the LUB. Decreasing rainfall, accordingly, would impact surface water resources by reducing their inflows. For the final climatic variable, the results of this study indicate that from 2000 to 2015, snowfall increased over the study area. However, after 2015, there was a decrease in snowfall in the LUB. Mountainous areas are mostly affected by snow, which can be seen in Figure 2.

5.4. Analysis of the Efficiency of the Applied JRC Global Surface Water Mapping Layers v1.4 for Surface Water Monitoring

Previous studies have predominantly utilized the MODIS land water mask (MOD44W) product for analyzing water areas [74–76]. This product delineates the boundary between land and water, encompassing both inland water bodies like rivers and lakes, as well as the ocean. However, it lacks the capability to differentiate between the ocean and inland water bodies, treating them as a single water entity. Moreover, it provides water area data at spatial resolutions of 250 and 500 m. Importantly, it does not offer detailed information on various surface water resources such as permanent and seasonal rivers. However, the applied JRC Global Surface Water Mapping Layers v1.4 in this study come with several advantages. This dataset encompasses maps delineating the location and temporal distribution of surface water from 1984 to 2021, offering insights into the extent and changes in surface waters, including permanent and seasonal rivers, lakes, seas, and oceans. Its high spatial resolution of 30 m enables precise detection and monitoring of all surface water resources on a large scale and over a long duration. Employing an expert

system, each pixel was individually classified into water or non-water, and the results were aggregated into a monthly historical record spanning the entire period and two epochs (1984–1999, 2000–2021) for change detection. This mapping layer product comprises a single image containing seven bands, mapping various aspects of the spatial and temporal distribution of surface water over the past 38 years. Areas where water has never been detected are appropriately masked.

5.5. Limitation of the Study

The primary constraint of this study stems from the temporal fluctuation inherent in the JRC Global Surface Water Mapping Layers v1.4 product. The absence of specific data regarding water surface storage for individual years presents a significant challenge. Comprehensive information delineating various facets of water surfaces, such as seasonal, temporal, monthly, and permanent reservoir data for each year separately, is crucial. Such data hold considerable value for monitoring shifts in water patterns over time.

6. Conclusions

This study investigated the impact of climate change and anthropogenic activities on surface water resources in the LUB from 2000 to 2020. The findings highlight the significant influence of both climate change and human activities on surface water resources. Furthermore, the study underscores the effectiveness of utilizing GEE in conjunction with remote sensing products like the JRC Global Surface Water Mapping Layers for monitoring spatio-temporal changes in surface water resources and assessing environmental impacts.

These findings provide valuable insights for decision-makers in semi-arid and arid regions like the LUB. By understanding the effects of climate change and anthropogenic variables on surface water resources, stakeholders can formulate more sustainable water management strategies. Given the success of this approach in the LUB, the research suggests applying similar methodologies to monitor surface water resources in other parts of the world facing similar challenges. Since the JRC product is available for a specific timeframe (1984–1999 and 2000–2021), the use of the MODIS water mask product could be explored to fill data gaps and provide a more comprehensive long-term perspective.

Author Contributions: M.K.G.: Conceptualization, Writing—original draft, Methodology. R.A.: Methodology, Investigation. S.A.C.: Formal analysis, Data curation, Conceptualization. M.S.A.: Writing—original draft, Validation. V.T. and S.L.: Review and editing, Supervision. A.S.: Methodology, Validation. All authors have read and agreed to the published version of the manuscript.

Funding: This research received no external funding.

Data Availability Statement: Data will be made available on reasonable request. The data are not available publicly due to ongoing research.

Conflicts of Interest: The authors declare that they have no known competing financial interests or personal relationships that could have appeared to influence the work reported in this paper.

References

1. Freudiger, D.; Kohn, I.; Stahl, K.; Weiler, M. Large-scale analysis of changing frequencies of rain-on-snow events with flood-generation potential. *Hydrol. Earth Syst. Sci.* **2014**, *18*, 2695–2709. [CrossRef]
2. Habibi, M.; Babaeian, I.; Schöner, W. Changing causes of drought in the Urmia Lake Basin—Increasing influence of evaporation and disappearing snow cover. *Water* **2021**, *13*, 3273. [CrossRef]
3. Masaeli, N.; Afshari, E.; Baniasadi, E.; Baharlou-Houreh, N.; Ghaedamini, M. Experimental analysis of water transfer and thermal–hydraulic performance of membrane humidifiers with three flow field designs. *Appl. Energy* **2023**, *336*, 120823. [CrossRef]
4. Fan, X.; Wang, L.; Li, X.; Zhou, J.; Chen, D.; Yang, H. Increased discharge across the Yellow River Basin in the 21st century was dominated by precipitation in the headwater region. *J. Hydrol. Reg. Stud.* **2022**, *44*, 101230. [CrossRef]
5. Abdelhalim, A.; Sefelnasr, A.; Ismail, E. Response of the interaction between surface water and groundwater to climate change and proposed megastructure. *J. Afr. Earth Sci.* **2020**, *162*, 103723. [CrossRef]
6. Wang, J.; Cui, C.; Jia, Z.; Liu, M.; Pang, S.; Zhai, K. Analysis of the responses of surface water resources to climate change in arid and semi-arid area. *Agric. Water Manag.* **2024**, *295*, 108751. [CrossRef]

7. Garajeh, M.K.; Feizizadeh, B. A comparative approach of data-driven split-window algorithms and MODIS products for land surface temperature retrieval. *Appl. Geomat.* **2021**, *13*, 715–733. [CrossRef]
8. Abdulla, F.; Al-Shurafat, A.W. Assessment of the impact of potential climate change on the surface water of a trans-boundary basin: Case study Yarmouk River. *Procedia Manuf.* **2020**, *44*, 172–179. [CrossRef]
9. Li, X.; Pu, X.; Wang, W.; Dong, X.; Zhang, Y.; Wang, J.; Wang, Y.; Meng, M. Surface water environmental carrying capacity and surface water quality based on economy-society-environment nexus–Evidence from China. *Water-Energy Nexus* **2023**, *6*, 231–243. [CrossRef]
10. Chen, L.; Liu, Y.; Li, J.; Tian, P.; Zhang, H. Surface water changes in China's Yangtze River Delta over the past forty years. *Sustain. Cities Soc.* **2023**, *91*, 104458. [CrossRef]
11. Wei, D.; Liu, S.; Wu, Y.; Feng, S.; Gao, H.; Qin, C.; Ren, D.; Tang, W.; Zhang, Y. Impacts of human activities and climate change on water and sediment evolution in four large subtropical river basins in China. *Ecol. Indic.* **2023**, *155*, 110958. [CrossRef]
12. He, X.; Guan, D.; Zhou, L.; Zhang, Y.; Gao, W.; Sun, L.; Huang, D.; Li, Z.; Cao, J.; Su, X. Quantifying spatiotemporal patterns and influencing factors of urban shrinkage in China within a multidimensional framework: A case study of the Yangtze River Economic Belt. *Sustain. Cities Soc.* **2023**, *91*, 104452. [CrossRef]
13. Kazemi Garajeh, M.; Weng, Q.; Hossein Haghi, V.; Li, Z.; Kazemi Garajeh, A.; Salmani, B. Learning-based methods for detection and monitoring of shallow flood-affected areas: Impact of shallow-flood spreading on vegetation density. *Can. J. Remote Sens.* **2022**, *48*, 481–503. [CrossRef]
14. Roth, V.; Lemann, T.; Zeleke, G.; Subhatu, A.T.; Nigussie, T.K.; Hurni, H. Effects of climate change on water resources in the upper Blue Nile Basin of Ethiopia. *Heliyon* **2018**, *4*, e00771. [CrossRef] [PubMed]
15. Tamm, O.; Maasikamäe, S.; Padari, A.; Tamm, T. Modelling the effects of land use and climate change on the water resources in the eastern Baltic Sea region using the SWAT model. *Catena* **2018**, *167*, 78–89. [CrossRef]
16. Li, X.; Zhang, Y.; Ma, N.; Li, C.; Luan, J. Contrasting effects of climate and LULC change on blue water resources at varying temporal and spatial scales. *Sci. Total Environ.* **2021**, *786*, 147488. [CrossRef]
17. Jin, T.; Zhang, X.; Wang, T.; Liang, J.; Ma, W.; Xie, J. Spatiotemporal impacts of climate change and human activities on blue and green water resources in northwest river basins of China. *Ecol. Indic.* **2024**, *160*, 111823. [CrossRef]
18. Shams Ghahfarokhi, M.; Moradian, S. Investigating the causes of Lake Urmia shrinkage: Climate change or anthropogenic factors? *J. Arid Land* **2023**, *15*, 424–438. [CrossRef]
19. Zeng, S.; Zhan, C.; Sun, F.; Du, H.; Wang, F. Effects of climate change and human activities on surface runoff in the Luan River Basin. *Adv. Meteorol.* **2015**, *2015*, 740239. [CrossRef]
20. Wang, Y.; Gu, X.; Yang, G.; Yao, J.; Liao, N. Impacts of climate change and human activities on water resources in the Ebinur Lake Basin, Northwest China. *J. Arid Land* **2021**, *13*, 581–598. [CrossRef]
21. Khelifa, R.; Mahdjoub, H.; Baaloudj, A.; Cannings, R.A.; Samways, M.J. Effects of both climate change and human water demand on a highly threatened damselfly. *Sci. Rep.* **2021**, *11*, 7725. [CrossRef] [PubMed]
22. He, T.; Xiao, W.; Zhao, Y.; Chen, W.; Deng, X.; Zhang, J. Continues monitoring of subsidence water in mining area from the eastern plain in China from 1986 to 2018 using Landsat imagery and Google Earth Engine. *J. Clean. Prod.* **2021**, *279*, 123610. [CrossRef]
23. Li, K.; Xu, E. High-accuracy continuous mapping of surface water dynamics using automatic update of training samples and temporal consistency modification based on Google Earth Engine: A case study from Huizhou, China. *ISPRS J. Photogramm. Remote Sens.* **2021**, *179*, 66–80. [CrossRef]
24. Mayer, T.; Poortinga, A.; Bhandari, B.; Nicolau, A.P.; Markert, K.; Thwal, N.S.; Markert, A.; Haag, A.; Kilbride, J.; Chishtie, F. Deep learning approach for Sentinel-1 surface water mapping leveraging Google Earth Engine. *ISPRS Open J. Photogramm. Remote Sens.* **2021**, *2*, 100005. [CrossRef]
25. Chen, Z.; Zhao, S. Automatic monitoring of surface water dynamics using Sentinel-1 and Sentinel-2 data with Google Earth Engine. *Int. J. Appl. Earth Obs. Geoinf.* **2022**, *113*, 103010. [CrossRef]
26. Liu, C.; Hu, R.; Wang, Y.; Lin, H.; Zeng, H.; Wu, D.; Liu, Z.; Dai, Y.; Song, X.; Shao, C. Monitoring water level and volume changes of lakes and reservoirs in the Yellow River Basin using ICESat-2 laser altimetry and Google Earth Engine. *J. Hydro-Environ. Res.* **2022**, *44*, 53–64. [CrossRef]
27. Katlane, R.; El Kilani, B.; Dhaoui, O.; Kateb, F.; Chehata, N. Monitoring of sea surface temperature, chlorophyll, and turbidity in Tunisian waters from 2005 to 2020 using MODIS imagery and the Google Earth Engine. *Reg. Stud. Mar. Sci.* **2023**, *66*, 103143. [CrossRef]
28. Pande, C.B.; Moharir, K.N.; Varade, A.M.; Abdo, H.G.; Mulla, S.; Yaseen, Z.M. Intertwined impacts of urbanization and land cover change on urban climate and agriculture in Aurangabad city (MS), India using google earth engine platform. *J. Clean. Prod.* **2023**, *422*, 138541. [CrossRef]
29. Ayyamperumal, R.; Banerjee, A.; Zhang, Z.; Nazir, N.; Li, F.; Zhang, C.; Huang, X. Quantifying climate variation and associated regional air pollution in southern India using Google Earth Engine. *Sci. Total Environ.* **2024**, *909*, 168470. [CrossRef]
30. Kazemi Garajeh, M.; Laneve, G.; Rezaei, H.; Sadeghnejad, M.; Mohamadzadeh, N.; Salmani, B. Monitoring trends of CO, NO_2, SO_2, and O_3 pollutants using time-series sentinel-5 images based on google earth engine. *Pollutants* **2023**, *3*, 255–279. [CrossRef]
31. Kazemi Garajeh, M. Monitoring the Spatio-Temporal Distribution of Soil Salinity Using Google Earth Engine for Detecting the Saline Areas Susceptible to Salt Storm Occurrence. *Pollutants* **2024**, *4*, 1–15. [CrossRef]

32. DEMİR, S.; BAŞAYİĞİT, L. Digital Mapping Burn Severity in Agricultural and Forestry Land over a Half-Decade Using Sentinel Satellite Images on the Google Earth Engine Platform: A Case Study in Isparta Province. *Trees For. People* **2024**, 100520. [CrossRef]
33. Huang, C.; Chen, Y.; Zhang, S.; Wu, J. Detecting, extracting, and monitoring surface water from space using optical sensors: A review. *Rev. Geophys.* **2018**, *56*, 333–360. [CrossRef]
34. Chang, H.-C.; Hsu, Y.-L.; Hung, S.-S.; Ou, G.-R.; Wu, J.-R.; Hsu, C. Autonomous water quality monitoring and water surface cleaning for unmanned surface vehicle. *Sensors* **2021**, *21*, 1102. [CrossRef]
35. Pekel, J.-F.; Cottam, A.; Gorelick, N.; Belward, A.S. High-resolution mapping of global surface water and its long-term changes. *Nature* **2016**, *540*, 418–422. [CrossRef] [PubMed]
36. Jin, H.; Fang, S.; Chen, C. Mapping of the Spatial Scope and Water Quality of Surface Water Based on the Google Earth Engine Cloud Platform and Landsat Time Series. *Remote Sens.* **2023**, *15*, 4986. [CrossRef]
37. Pickens, A.H.; Hansen, M.C.; Hancher, M.; Stehman, S.V.; Tyukavina, A.; Potapov, P.; Marroquin, B.; Sherani, Z. Mapping and sampling to characterize global inland water dynamics from 1999 to 2018 with full Landsat time-series. *Remote Sens. Environ.* **2020**, *243*, 111792. [CrossRef]
38. Jones, J.W. Improved automated detection of subpixel-scale inundation—Revised dynamic surface water extent (DSWE) partial surface water tests. *Remote Sens.* **2019**, *11*, 374. [CrossRef]
39. Schulz, S.; Darehshouri, S.; Hassanzadeh, E.; Tajrishy, M.; Schüth, C. Climate change or irrigated agriculture–what drives the water level decline of Lake Urmia. *Sci. Rep.* **2020**, *10*, 236. [CrossRef]
40. Abbasian, M.S.; Najafi, M.R.; Abrishamchi, A. Increasing risk of meteorological drought in the Lake Urmia basin under climate change: Introducing the precipitation–temperature deciles index. *J. Hydrol.* **2021**, *592*, 125586. [CrossRef]
41. Shirmohammadi, B.; Malekian, A.; Salajegheh, A.; Taheri, B.; Azarnivand, H.; Malek, Z.; Verburg, P.H. Scenario analysis for integrated water resources management under future land use change in the Urmia Lake region, Iran. *Land Use Policy* **2020**, *90*, 104299. [CrossRef]
42. Feizizadeh, B.; Garajeh, M.K.; Lakes, T.; Blaschke, T. A deep learning convolutional neural network algorithm for detecting saline flow sources and mapping the environmental impacts of the Urmia Lake drought in Iran. *Catena* **2021**, *207*, 105585. [CrossRef]
43. Ghale, Y.A.G.; Baykara, M.; Unal, A. Investigating the interaction between agricultural lands and Urmia Lake ecosystem using remote sensing techniques and hydro-climatic data analysis. *Agric. Water Manag.* **2019**, *221*, 566–579. [CrossRef]
44. Garajeh, M.K.; Malakyar, F.; Weng, Q.; Feizizadeh, B.; Blaschke, T.; Lakes, T. An automated deep learning convolutional neural network algorithm applied for soil salinity distribution mapping in Lake Urmia, Iran. *Sci. Total Environ.* **2021**, *778*, 146253. [CrossRef] [PubMed]
45. Muñoz Sabater, J. *ERA5-Land Monthly Averaged Data from 1981 to Present [Dataset]*; Copernicus Climate Change Service (C3S) Climate Data Store (CDS): Brussels, Belgium, 2019. [CrossRef]
46. Saha, S.; Moorthi, S.; Wu, X.; Wang, J.; Nadiga, S.; Tripp, P.; Behringer, D.; Hou, Y.; Chuang, H.; Iredell, M. *Updated daily. NCEP Climate Forecast System Version 2 (CFSv2) 6-Hourly Products*; Research Data Archive at the National Center for Atmospheric Research, Computational and Information Systems Laboratory: Boulder, CO, USA, 2011. [CrossRef]
47. Hall, D.; Riggs, G.; Salomonson, V. *MODIS/Terra Snow Cover Daily L3 Global 500m Grid, Version 6*; NASA National Snow and Ice Data Center Distributed Active Archive Center: Boulder, CO, USA, 2016.
48. Adler, R.F.; Huffman, G.J.; Chang, A.; Ferraro, R.; Xie, P.-P.; Janowiak, J.; Rudolf, B.; Schneider, U.; Curtis, S.; Bolvin, D. The version-2 global precipitation climatology project (GPCP) monthly precipitation analysis (1979–present). *J. Hydrometeorol.* **2003**, *4*, 1147–1167. [CrossRef]
49. Pesaresi, M.; Politis, P. *GHS-BUILT-S R2023A-GHS Built-Up Surface Grid, Derived from Sentinel2 Composite and Landsat, Multitemporal (1975–2030) [Dataset]*; European Commission, Joint Research Centre (JRC): Luxembourg, 2023.
50. Feizizadeh, B.; Lakes, T.; Omarzadeh, D.; Sharifi, A.; Blaschke, T.; Karimzadeh, S. Scenario-based analysis of the impacts of lake drying on food production in the Lake Urmia Basin of Northern Iran. *Sci. Rep.* **2022**, *12*, 6237. [CrossRef] [PubMed]
51. Gorelick, N.; Hancher, M.; Dixon, M.; Ilyushchenko, S.; Thau, D.; Moore, R. Google Earth Engine: Planetary-scale geospatial analysis for everyone. *Remote Sens. Environ.* **2017**, *202*, 18–27. [CrossRef]
52. Hamed, K.H.; Rao, A.R. A modified Mann-Kendall trend test for autocorrelated data. *J. Hydrol.* **1998**, *204*, 182–196. [CrossRef]
53. Kim, S. ppcor: An R package for a fast calculation to semi-partial correlation coefficients. *Commun. Stat. Appl. Methods* **2015**, *22*, 665. [CrossRef]
54. Irannezhad, M.; Ahmadian, S.; Sadeqi, A.; Minaei, M.; Ahmadi, B.; Marttila, H. Peak spring flood discharge magnitude and timing in natural rivers across northern Finland: Long-term variability, trends, and links to climate teleconnections. *Water* **2022**, *14*, 1312. [CrossRef]
55. Helsel, D.R.; Hirsch, R.M. *Statistical Methods in Water Resources*; Elsevier: Amsterdam, The Netherlands, 1993.
56. Sadeqi, A.; Tabari, H.; Dinpashoh, Y. Spatio-temporal analysis of heating and cooling degree-days over Iran. *Stoch. Environ. Res. Risk Assess.* **2022**, *36*, 869–891. [CrossRef]
57. Alizadeh-Choobari, O.; Ahmadi-Givi, F.; Mirzaei, N.; Owlad, E. Climate change and anthropogenic impacts on the rapid shrinkage of Lake Urmia. *Int. J. Climatol.* **2016**, *36*, 4276–4286. [CrossRef]
58. Ebrahimi Sirizi, M.; Taghavi Zirvani, E.; Esmailzadeh, A.; Khosravian, J.; Ahmadi, R.; Mijani, N.; Soltannia, R.; Jokar Arsanjani, J. A Scenario-Based Multi-Criteria Decision-Making Approach for Allocation of Pistachio Processing Facilities: A Case Study of Zarand, Iran. *Sustainability* **2023**, *15*, 15054. [CrossRef]

59. Hasemi, M. *A Socio-Technical Assessment Framework for Integrated Water Resources Management (IWRM) in Lake Urmia Basin, Iran*; Newcastle University: Newcastle upon Tyre, UK, 2011.
60. Chaudhari, S.; Felfelani, F.; Shin, S.; Pokhrel, Y. Climate and anthropogenic contributions to the desiccation of the second largest saline lake in the twentieth century. *J. Hydrol.* **2018**, *560*, 342–353. [CrossRef]
61. Safari, H.; Montaseri, M.; Hejabi, S. Spatiotemporal changes in snow cover and their relationship with drought events in the Lake Urmia basin. *Hydrol. Sci. J.* **2024**, *69*, 46–62. [CrossRef]
62. Kazemi Garajeh, M.; Haji, F.; Tohidfar, M.; Sadeqi, A.; Ahmadi, R.; Kariminejad, N. Spatiotemporal monitoring of climate change impacts on water resources using an integrated approach of remote sensing and Google Earth Engine. *Sci. Rep.* **2024**, *14*, 5469. [CrossRef] [PubMed]
63. Harati, H.; Kiadaliri, M.; Tavana, A.; Rahnavard, A.; Amirnezhad, R. Urmia Lake dust storms occurrences: Investigating the relationships with changes in water zone and land cover in the eastern part using remote sensing and GIS. *Environ. Monit. Assess.* **2021**, *193*, 70. [CrossRef] [PubMed]
64. Kordi, F.; Yousefi, H. Crop classification based on phenology information by using time series of optical and synthetic-aperture radar images. *Remote Sens. Appl. Soc. Environ.* **2022**, *27*, 100812. [CrossRef]
65. Ghaheri, M.; Baghal-Vayjooee, M.; Naziri, J. Lake Urmia, Iran: A summary review. *Int. J. Salt Lake Res.* **1999**, *8*, 19–22. [CrossRef]
66. Fathian, F.; Morid, S.; Kahya, E. Identification of trends in hydrological and climatic variables in Urmia Lake basin, Iran. *Theor. Appl. Climatol.* **2015**, *119*, 443–464. [CrossRef]
67. Hassanzadeh, E.; Zarghami, M.; Hassanzadeh, Y. Determining the main factors in declining the Urmia Lake level by using system dynamics modeling. *Water Resour. Manag.* **2012**, *26*, 129–145. [CrossRef]
68. Torabi Haghighi, A.; Fazel, N.; Hekmatzadeh, A.A.; Klöve, B. Analysis of effective environmental flow release strategies for Lake Urmia restoration. *Water Resour. Manag.* **2018**, *32*, 3595–3609. [CrossRef]
69. Danesh-Yazdi, M.; Ataie-Ashtiani, B. Lake Urmia crisis and restoration plan: Planning without appropriate data and model is gambling. *J. Hydrol.* **2019**, *576*, 639–651. [CrossRef]
70. Kabiri, K.; Pradhan, B.; Sharifi, A.; Ghobadi, Y.; Pirasteh, S. Manifestation of remotely sensed data coupled with field measured meteorological data for an assessment of degradation of Urmia Lake, Iran. In Proceedings of the Asia Pacific Conference on Environmental Science and Technology, APEST, Kuala Lumpur, Malaysia, 1–2 February 2012; pp. 395–401.
71. Mansourihanis, O.; Maghsoodi Tilaki, M.J.; Yousefian, S.; Zaroujtaghi, A. A Computational Geospatial Approach to Assessing Land-Use Compatibility in Urban Planning. *Land* **2023**, *12*, 2083. [CrossRef]
72. Khosravian, J.; Qureshi, S.; Rostamzadeh, S.; Moradi, B.; Derakhshesh, P.; Yousefi, S.; Jamali, K.; Ahmadi, R.; Nickravesh, F. Evaluating the feasibility of constructing shopping centers on urban vacant land through a spatial multi-criteria decision-making model. *Front. Sustain. Cities* **2024**, *6*, 1373331. [CrossRef]
73. Kazemi Garajeh, M.; Salmani, B.; Zare Naghadehi, S.; Valipoori Goodarzi, H.; Khasraei, A. An integrated approach of remote sensing and geospatial analysis for modeling and predicting the impacts of climate change on food security. *Sci. Rep.* **2023**, *13*, 1057. [CrossRef] [PubMed]
74. Carroll, M.L.; Townshend, J.R.; DiMiceli, C.M.; Noojipady, P.; Sohlberg, R.A. A new global raster water mask at 250 m resolution. *Int. J. Digit. Earth* **2009**, *2*, 291–308. [CrossRef]
75. Sharma, R.C.; Tateishi, R.; Hara, K.; Nguyen, L.V. Developing superfine water index (SWI) for global water cover mapping using MODIS data. *Remote Sens.* **2015**, *7*, 13807–13841. [CrossRef]
76. Li, L.; Vrieling, A.; Skidmore, A.; Wang, T.; Turak, E. Monitoring the dynamics of surface water fraction from MODIS time series in a Mediterranean environment. *Int. J. Appl. Earth Obs. Geoinf.* **2018**, *66*, 135–145. [CrossRef]